ACS Catalysis

Research Article

pubs.acs.org/acscatalysis

Simultaneous and Stoichiometric Water Oxidation and Cr(VI) Reduction in Aqueous Suspensions of Functionalized Plasmonic Photocatalyst Au/TiO_2−Pt under Irradiation of Green Light

Atsuhiro Tanaka, Kousuke Nakanishi, Ryosuke Hamada, Keiji Hashimoto, and Hiroshi Kominami*

Department of Applied Chemistry, Faculty of Science and Engineering, Kinki University Kowakae, Higashiosaka, Osaka 577-8502 Japan

ABSTRACT: Titanium(IV) oxide (TiO_2) having both small platinum (Pt) nanoparticles and large gold (Au) particles without alloying and nanoparticle coagulation was successfully prepared by the combination of traditional photodeposition of Pt and subsequent Au colloid photodeposition onto TiO_2−Pt. The Au/TiO_2 and Au/TiO_2−Pt samples exhibiting strong photoabsorption due to surface plasmon resonance (SPR) of supported Au particles were used for the reduction of hexavalent chromium (Cr^{6+} in $Cr_2O_7^{2-}$) in aqueous suspensions under irradiation of visible light from a green light emitting diode (LED). These SPR-type photocatalysts reduced Cr^{6+} and evolved dioxygen (O_2) with O_2-reduced Cr^{6+} ratio of 3:4 until consumption of Cr^{6+}, indicating that these SPR-type photocatalysts had the ability to oxidize water (H_2O) utilizing visible light (λ = 540 nm) and that a photocatalytic reaction ($2Cr_2O_7^{2-} + 16H^+ \rightarrow 4Cr^{3+} + 3O_2 + 8H_2O$) occurred. The Au/$TiO_2$−Pt sample exhibited a reaction rate about twice larger than that of Pt-free Au/TiO_2, and the apparent quantum yield reached 1.0% at 550 nm and 0.47% even at 700 nm, indicating that functionalization of Au/TiO_2 was successfully achieved by introduction of a Pt cocatalyst. This reaction can be used as a test reaction for evaluation of O_2 evolution ability of photocatalysts because this reaction does not induce irreversible changes in photocatalysts.

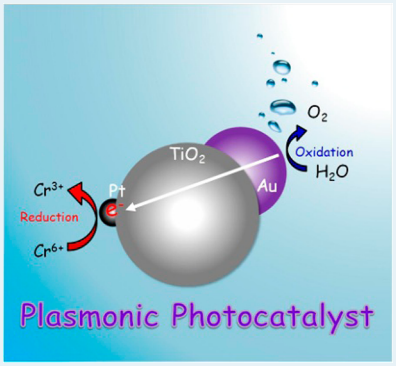

KEYWORDS: *photocatalyst, reduction reaction, gold nanoparticles, surface plasmon resonance, visible light*

1. INTRODUCTION

Oxidation of water (H_2O) to dioxygen (O_2) in photosynthesis is one of the most important and fundamental chemical processes in nature.[1] There have been numerous attempts to develop artificial photosynthesis since it would eventually lead to the production of solar fuels.[2] In overall H_2O splitting, hydrogen in H_2O (or proton (H^+)) is reduced by electrons to form dihydrogen (H_2), and oxygen in H_2O is oxidized by holes to form O_2. Production of H_2 by semiconductor photocatalysts under irradiation of visible light has attracted much attention because it offers a promising way for clean, low-cost, and environmentally friendly production of H_2 by solar light. On the other hand, comparing the two half-reactions of overall water splitting, O_2 formation is considered to be more difficult than H_2 formation since mechanistically it has to occur through several steps requiring four positive holes and the formation of O−O bonds.[3] In general, photocatalytic O_2 formation from H_2O is examined in the presence of a sacrificial electron acceptor, and silver salts (nitrate and sulfate) were used entirely as the electron acceptor. During photocatalytic O_2 formation, silver ions are reduced to silver metal (Ag) and Ag particles are deposited on the surface of the photocatalyst. Since the surface of the photocatalyst is covered with Ag particles and the Ag particles shield the light, the reaction rate gradually decreases with prolongation of the reaction time.[4] Therefore, it is impossible to perform durability tests of photocatalysts, that is, photocatalytic reactions for long time duration and reuse experiments.

Recently, gold (Au) nanoparticles supported on titanium(IV) oxide (TiO_2) and cerium(IV) oxide exhibiting surface plasmon resonance (SPR) have been applied to a visible light-responding photocatalyst for various chemical reactions,[5,6] that is, oxidation of organic substrates, selective oxidation of aromatic alcohol to a carbonyl compound, hydrogen formation from alcohols, and selective reduction of organic compounds. When O_2 evolution induced by photoabsorption due to SPR of metal nanoparticles is evaluated, silver salts cannot be used as electron scavengers because the photoabsorption properties continuously change because of direct deposition of Ag onto Au nanoparticles. Ag-deposited Au/TiO_2 is a different photocatalyst, and its activity should not be compared with that of a fresh photocatalyst (Ag-free Au/TiO_2). Therefore, it is impossible to obtain information on stability and durability of photocatalysts utilizing photoabsorption due to SPR if silver salts are used as electron scavengers. Another convenient reaction system is required to evaluate stability and durability of photocatalysts for O_2 formation (H_2O oxidation), especially SPR-type photocatalysts.

Received: June 6, 2013
Revised: July 10, 2013
Published: July 11, 2013

As an alternative, we anticipate that the reduction of hexavalent chromium (Cr^{6+} in $Cr_2O_7^{2-}$) to trivalent chromium (Cr^{3+}) along with oxidation of H_2O to O_2 is a promising reaction system to evaluate activity for O_2 formation free from change in photoabsorption of an SPR-photocatalyst. Yoneyama et al. studied the reduction of Cr^{6+} at acid pH using heterogeneous photocatalysts (such as TiO_2, WO_3, Fe_2O_3, and $SrTiO_3$).[7] Cr^{6+} was reduced to Cr^{3+} by photogenerated electrons as shown in eq 1.

$$Cr_2O_7^{2-} + 14H^+ + 6e^- \rightarrow 2Cr^{3+} + 7H_2O \quad (1)$$

As shown in eq 2, water scavenges six holes and six photogenerated electrons can be used for reduction of Cr^{6+}.

$$3H_2O + 6h^+ \rightarrow \frac{3}{2}O_2 + 6H^+ \quad (2)$$

In total, the photocatalytic reaction is expressed as eq 3.

$$Cr_2O_7^{2-} + 8H^+ \rightarrow 2Cr^{3+} + \frac{3}{2}O_2 + 4H_2O \quad (3)$$

Since Cr^{3+} is soluble in H_2O at low pH[8], it is expected that formation of Cr^{3+} does not alter the photoabsorption of the photocatalyst and the photocatalytic activity for oxidation of H_2O in contrast to the Ag^+-Ag reaction system.

In our previous study,[6h,i] we found that TiO_2 having both small metal nanoparticles and large Au particles without alloying and nanoparticle coagulation could be successfully prepared by the combination of traditional photodeposition of metal in the presence of a hole scavenger (PH) and subsequent Au colloid photodeposition in the presence of a hole scavenger (CPH)[6g] onto TiO_2 metal. The functionalized Au/TiO_2 samples with a platinum (Pt) cocatalyst and silver (Ag), that is, Au/TiO_2−Pt and Au/TiO_2−Ag, exhibited much larger rates of H_2 formation and nitrobenzene reduction than those of the metal-free Au/TiO_2 sample. Therefore, functionalization of Au/TiO_2 samples with a cocatalyst is an effective method for enhancing performance, especially when electron scavenging is important.

In this study, we used an Au/TiO_2 sample for photocatalytic reduction of Cr^{6+} and oxidation of H_2O without using reducing reagents under irradiation of visible light. Here we report that photocatalytic reduction of Cr^{6+} to Cr^{3+} along with oxidation of H_2O to O_2 under irradiation of visible light was achieved and that the photocatalytic performance was drastically improved by functionalization of Au/TiO_2 with Pt nanoparticles as a cocatalyst.

2. EXPERIMENTAL SECTION

2.1. Preparation of Samples. Loading of 0.5 wt % Pt nanoparticles on TiO_2 (preparation of TiO_2−Pt) was performed by the PH method. TiO_2 powder was suspended in 10 cm^3 of an aqueous solution of methanol (50 vol%) in a test tube, and the test tube was sealed with a rubber septum under argon (Ar). An aqueous solution of hexachloroplatinic-(IV) acid (H_2PtCl_6) as a metal source was injected into the sealed test tube and then photoirradiated for 1 h at $\lambda > 300$ nm by a 400-W high-pressure mercury arc (Eiko-sha, Osaka) with magnetic stirring in a water bath continuously kept at 298 K. The Pt source was reduced by photogenerated electrons and Pt was deposited on the surface of TiO_2 particles. Analysis of the liquid phase after photodeposition revealed that the Pt source had been almost completely (>99.9%) deposited on the TiO_2 particles. The resultant powder was washed repeatedly with distilled water and then dried at 310 K overnight under air.

Colloidal Au nanoparticles were prepared using the method reported by Frens.[9] To 750 cm^3 of an aqueous tetrachloroauric-(III) acid ($HAuCl_4$) solution (0.49 mmol dm^{-3}), 100 cm^3 of an aqueous solution containing sodium citrate (39 mmol dm^{-3}) was added. The solution was heated and boiled for 1 h. After the color of the solution had changed from deep blue to deep red, the solution was boiled for a further 30 min. After cooling the solution to room temperature, Amberlite MB-1 (ORGANO, 60 cm^3) was added to remove excess sodium citrate. After 1 h treatment, MB-1 was removed from the solution using a glass filter. Loading of 1.0 wt % Au particles on the TiO_2−Pt samples was performed by the CPH method.[6g] A TiO_2−Pt sample (168 mg) was suspended in 20 cm^3 of an aqueous solution of colloidal Au nanoparticles (0.085 mg cm^{-3}) in a test tube, and the test tube was sealed with a rubber septum under Ar. An aqueous solution of oxalic acid (50 μmol) was injected into the sealed test tube. The mixture was photoirradiated at $\lambda > 300$ nm by a 400 W high-pressure mercury arc under Ar with magnetic stirring in a water bath continuously kept at 298 K. The resultant powder was washed repeatedly with distilled water and then dried at 310 K overnight under air. Pt-free samples (Au/TiO_2) were also prepared by the same method using bare TiO_2 samples. Hereafter, an Au-loaded TiO_2−Pt sample is designated as Au/TiO_2−Pt. Morphology of the samples was observed under a JEOL JEM-3010 transmission electron microscope (TEM) operated at 300 kV in the Joint Research Center of Kinki University.

2.2. Photocatalytic Reaction. The dried photocatalyst powder (50 mg) was suspended in an aqueous solution (5 cm^3) containing $K_2Cr_2O_7$ in a test tube with the initial concentration set at 1 mM, and pH was adjusted to 2 with H_2SO_4. The solution was bubbled with Ar, and the test tube was sealed with a rubber septum. The suspension was irradiated with visible light of a green light emitting diode (LED) with magnetic stirring at 298 K. The amount of O_2 in the gas phase was measured using a Shimadzu GC-8A gas chromatograph equipped with an MS-5A column. The concentration of Cr^{6+} was determined using the colorimetric method that uses 1,5-diphenycarbazide reagent.[10] The color change was monitored at 542 nm using a UV−visible spectrophotometer (UV-2400, Shimadzu, Kyoto). In some experiments, the concentration of total soluble chromium was also determined using the same colorimetric method, in which oxidation of chromium species having oxidation states lower than +VI by using potassium permanganate was carried out as pretreatment. The concentration of total chromium after the photocatalytic reaction was the same as that before the reaction, indicating that all chromium species were dissolved in the present reaction conditions. In this study, the concentration of Cr^{3+} was determined from the difference between the concentrations of Cr^{6+} before and after the reaction.

3. RESULTS AND DISCUSSION

3.1. Characterization of TiO_2−Pt, Au/TiO_2, and Au/TiO_2−Pt. Figure 1a shows a TEM image of a sample of TiO_2 with 0.5 wt % Pt cocatalyst (TiO_2−Pt) simply prepared by the traditional PH method. Small Pt particles were observed and the average diameter was determined to be 3.0 nm, indicating that the Pt nanoparticles were successfully deposited on the surface of TiO_2 by using the PH method (Figure 2a). Figure 1b shows a TEM image of colloidal Au nanoparticles, revealing

dx.doi.org/10.1021/cs400433r | ACS Catal. 2013, 3, 1886−1891

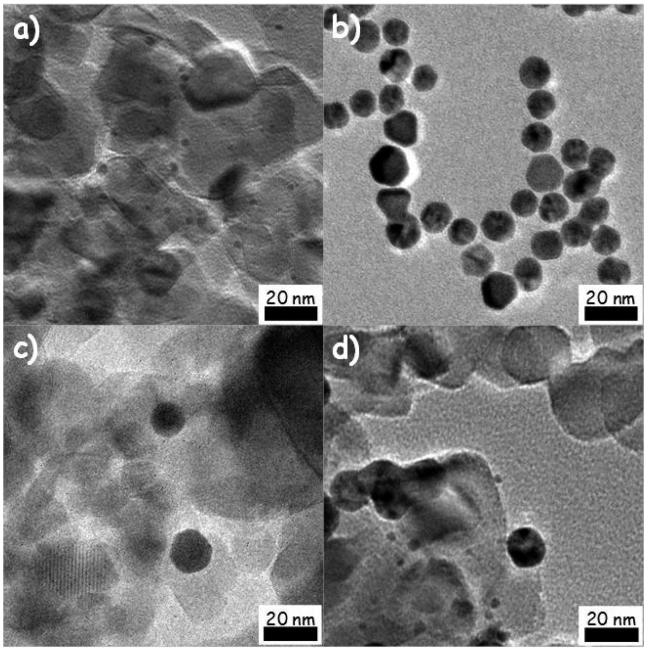

Figure 1. TEM images of (a) TiO_2–Pt(0.5), (b) colloidal Au nanoparticles, (c) Au(1.0)/TiO_2, and (d) Au(1.0)/TiO_2–Pt(0.5).

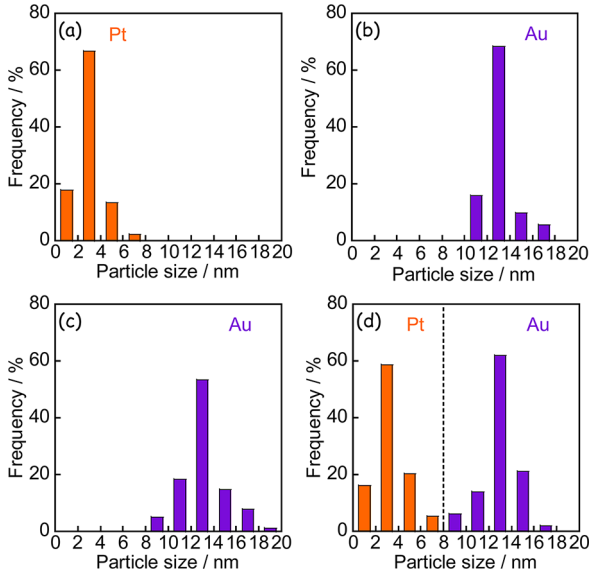

Figure 2. Size distributions of (a) TiO_2–Pt (0.5 wt %), (b) colloidal Au nanoparticles, (c) Au (1.0 wt %)/TiO_2, and (d) Au (1.0 wt %)/TiO_2–Pt (0.5 wt %).

that Au nanoparticles have an average particle size of 13 nm within a relatively sharp distribution with a standard deviation of 1.4 nm (Figure 2b). Figure 1c shows a TEM image of TiO_2 with 1.0 wt % Au nanoparticles (Au/TiO_2) prepared by the CPH method using the Au colloidal solution. Gold particles were observed in the image, indicating that Au nanoparticles were deposited on the TiO_2 surface by the CPH method. The average diameter of Au particles of the sample was determined to be 13 nm, which was in good agreement with the average diameter of original colloidal Au nanoparticles before Au loading (Figure 1b, Figure 2c).

By using the CPH method, Au nanoparticles (1.0 wt %) were introduced on the TiO_2–Pt sample, and Figure 1d shows a TEM image of the Au/TiO_2–Pt sample, indicating the presence of both smaller particles and larger particles with average diameters determined to be 3.3 and 13 nm, respectively (Figure 2d). From the TEM images of TiO_2–Pt and Au/TiO_2 samples, the smaller and larger particles of the Au/TiO_2–Pt sample were assigned to Pt and Au, respectively. These results indicate that the CPH method induced no change in Pt nanoparticles during loading of Au particles and that Au nanoparticles were successfully loaded on TiO_2–Pt without change in the original particle size as in the case of loading of Au onto bare TiO_2. In our previous study using the CPH method, we found that the presence of a hole scavenger was indispensable for quantitative loading of Au particles, that is, a reductive condition should be created on the TiO_2 surface.[6g] Therefore, in the case of loading of Au particles on TiO_2–Pt by the CPH method, Au particles were probably deposited in contact with Pt nanoparticles because Pt particles loaded on TiO_2 often act as reduction sites in various reaction systems. The numbers of Pt and Au particles in TiO_2–Pt and Au/TiO_2 samples were calculated to be 1.2×10^{16} and 4.5×10^{14} per g-TiO_2, respectively, from the average sizes, contents, and densities of Pt and Au assuming that both Pt and Au particles were spherical. Since the number of Pt particles was much larger than that of Au particles, the decrease in the number of exposed Pt particles because of contact with Au particles by the CPH method is negligible in the Au/TiO_2–Pt sample.

Figure 3 shows absorption spectra of the TiO_2, TiO_2–Pt(0.5), Au(1.0)/TiO_2, and Au(1.0)/TiO_2–Pt(0.5) samples for which TEM images are shown in Figure 1. The bare TiO_2 sample exhibited only an absorption at $\lambda < 400$ nm due to the band gap excitation. Loading Pt nanoparticles onto TiO_2 resulted in an increase in the baseline of photoabsorption that has generally been observed as change in color from white to gray. In the spectra of Au(1.0)/TiO_2 and Au(1.0)/TiO_2–Pt(0.5) samples, strong photoabsorption was observed at around 550 nm, which was attributed to SPR of the supported Au nanoparticles.[5,6]

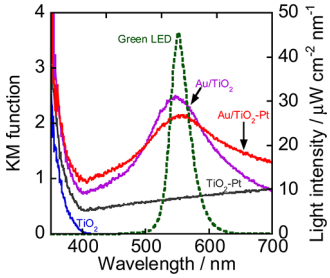

Figure 3. Absorption spectra of TiO_2, TiO_2–Pt(0.5), Au(1.0)/TiO_2, and Au(1.0)/TiO_2–Pt(0.5) samples and visible light irradiated to reaction systems from a green LED.

3.2. Photocatalytic Reaction. The photocatalytic activity of Au/TiO_2–Pt was evaluated in the reduction of Cr^{6+} (initially 10 μmol) along with H_2O oxidation. Figure 4a shows the time courses of photocatalytic reduction of Cr^{6+} to Cr^{3+} and oxidation of H_2O to O_2 in an aqueous suspension of Au/TiO_2–Pt under irradiation of visible light from a green LED. Visible light irradiated to the reaction system is shown in Figure 3. The amount of Cr^{6+} decreased linearly with photoirradiation, while Cr^{3+} as the reduction product of Cr^{6+} and O_2 as the oxidation product of H_2O formed corresponding to the decrease in amount of Cr^{6+}. It should be noted that the plot of Cr^{3+} always

dx.doi.org/10.1021/cs400433r | ACS Catal. 2013, 3, 1886–1891

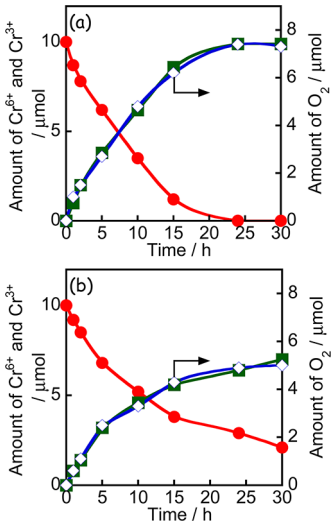

Figure 4. Time courses of the amounts of Cr^{6+} (closed circles), Cr^{3+} (closed squares), and O_2 (open diamonds) in aqueous suspensions of (a) Au/TiO_2−Pt and (b) Au/TiO_2 under irradiation of visible light from a green LED.

overlapped with the plot of O_2 almost completely in Figure 4a (scale in the right axis for O_2 being three-fourths that in the left axis), indicating that this photocatalytic reaction occurred with maintenance of high stoichiometry shown in eq 3. Cr^{6+} was completely consumed after irradiation for 24 h, while 10 μmol of Cr^{3+} was formed as the reduced product. The amount of Cr^{3+} (10 μmol) after photoirradiation for 24 h was about 4.0- and was 7.7-times larger than the amounts of Au (2.5 μmol) and Pt (1.3 μmol) loaded on TiO_2, indicating that the reduction of Cr^{6+} observed in the present study was a (photo)catalytic reaction. The result indicates that Cr^{3+} was formed with a quite high selectivity (>99%) at >99% conversion of Cr^{6+}, that is, quantitative conversion of Cr^{6+} to Cr^{3+} was achieved, in the present photocatalytic reaction system under irradiation of visible light. We also confirmed that further irradiation to the reaction mixture did not alter the amount of Cr^{3+} (Figure 4a).

To clarify the effect of Pt nanoparticles on this reaction, the Pt-free Au/TiO_2 sample shown in Figure 1c was also used under the same conditions, and the results are shown in Figure 4b. Stoichiometric formation of Cr^{3+} and O_2 was also observed in the case of the Pt-free Au/TiO_2 sample; however, the reaction rate was smaller (ca. 55%) than that of the Au/TiO_2−Pt sample. These results indicate that the reduction of Cr^{6+} was the rate-determining step in the Pt-free Au/TiO_2 sample, and Pt nanoparticles acted as a cocatalyst in this reaction system.

An action spectrum is a strong tool for determining whether a reaction observed occurs via a photoinduced process or a thermocatalytic process. To obtain an action spectrum in this reaction system, Cr^{6+} reduction in aqueous suspensions of $Au(1.0)/TiO_2$−$Pt(0.5)$ was carried out at 298 K under irradiation of monochromated visible light from a Xe lamp with light width of ±5 nm. Apparent quantum efficiency (AQE) at each centered wavelength of light was calculated from the ratio of the triple amount of Cr^{6+} reduction and the amount of photons irradiated using the following equation

$$\mathrm{AQE} = \frac{3 \times \text{the amount of } Cr^{6+} \text{ reduced}}{\text{the amount of incident photons}} \times 100$$

As shown in Figure 5, AQE was in agreement with the subtraction spectrum obtained from the spectra of $Au(1.0)/TiO_2$−$Pt(0.5)$ and TiO_2−$Pt(0.5)$. Therefore, it can be concluded that Cr^{6+} reduction in an aqueous suspension of $Au(1.0)/TiO_2$−$Pt(0.5)$ was induced by photoabsorption due to SPR of Au supported on TiO_2. We noted that AQE reached 1.0% at 550 nm and 0.47% even at 700 nm under the above conditions in the case of $Au(1.0)/TiO_2$−$Pt(0.5)$. Maeda and Domen reported the $BaZrO_3$−$BaTaO_2N$ solid-solution photocatalyst as one of the most efficient materials for water oxidation to O_2.[11] The longest wavelength of light inducing the reaction was 660 nm, which corresponded to the absorption edge of $BaZrO_3$−$BaTaO_2N$. Therefore, it is clear that the present Au/TiO_2−Pt is an excellent H_2O oxidation photocatalyst working under irradiation of light (λ = 700 nm) that did not excite any other photocatalysts for H_2O oxidation.

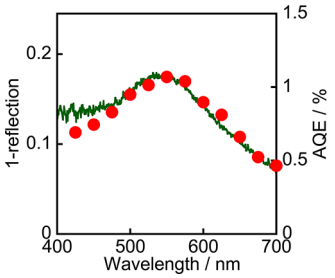

Figure 5. Subtraction spectrum obtained from spectra of $Au(1.0)/TiO_2$−$Pt(0.5)$ and TiO_2−$Pt(0.5)$ measured with barium sulfate as a reference (left axis), and the action spectrum of $Au(1.0)/TiO_2$−$Pt(0.5)$ (circles) in the reduction of Cr^{6+} (right axis).

The present Au/TiO_2−Pt sample was easily recovered from the reaction mixture after photoirradiation by simple filtration and was found to be reusable without loss of its activity; the amounts of O_2 formation after irradiation for 24 h were the same in both the second and the third uses of the Au/TiO_2−Pt sample (Figure 6a). In addition, as shown in Figure 7a and b,

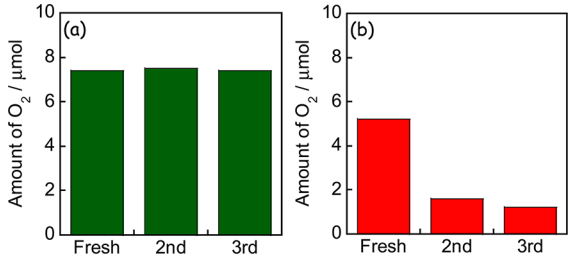

Figure 6. Amount of O_2 after irradiation for 24 h in oxidation of water in aqueous suspensions of Au/TiO_2−Pt in the presence of (a) Cr^{6+} and (b) Ag^+ under irradiation of visible light from a green LED.

photoabsorption of the Au/TiO_2−Pt sample scarcely changed even after this reaction. For comparison, we examined the oxidation of H_2O to O_2 over the Au/TiO_2−Pt sample in the presence of silver nitrate ($AgNO_3$) (6 mmol dm^{-3}) under irradiation of green light from an LED and a reusable test. Figure 6b shows the amount of O_2 evolved after irradiation for 24 h. The O_2 formation activity decreased with increase in the number of cycles, and photoabsorption of Au/TiO_2−Pt after the reaction was much different from that of the original Au/TiO_2−Pt as shown in Figure 7c, indicating that deposition of Ag metal drastically altered the photoabsorption property of the

dx.doi.org/10.1021/cs400433r | ACS Catal. 2013, 3, 1886−1891

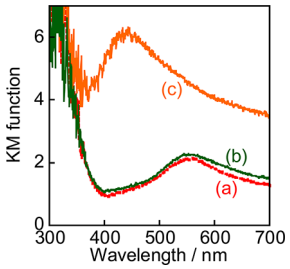

Figure 7. Absorption spectra of Au/TiO_2−Pt samples: (a) fresh sample, (b) after photocatalytic oxidation of H_2O to O_2 in the presence of Cr^{6+} for 24 h, and (c) after photocatalytic oxidation of H_2O to O_2 in the presence of Ag^+ ($AgNO_3$) for 24 h.

original Au/TiO_2−Pt. The results of two O_2 evolution systems indicate that Au/TiO_2 and Au/TiO_2−Pt have enough potential to oxidize H_2O (H_2O/O_2: 1.23 V_{NHE} pH0) and that the present reaction system can be used for evaluation of photocatalytic activity in H_2O oxidation without changes in the photoabsorption property and the activity of the photocatalyst. As shown above, the overall reaction rate of the Pt-free Au/TiO_2 sample is determined by the rate for Cr^{6+} reduction. Therefore, we should pay attention when we compare the activities of various photocatalysts because the rate-determining steps may be different.

The concentration of Cr^{6+} is easily determined by using a colorimetric method as well as the amount of O_2 determined by gas chromatography. Based on the results of Cr^{6+} reduction and O_2 evolution, the stoichiometry of the reaction, that is, balance of electron consumption and hole consumption (redox balance), can be checked. If the balance is different from the stoichiometry, some noncatalytic process such as changes in the photocatalyst occurs. In the cases of Au/TiO_2−Pt and Au/TiO_2, the balance of products satisfies the stoichiometry as discussed.

Results of Cr^{6+} reduction over various photocatalysts under green light from an LED are shown in Figure 8. No Cr^{6+} was

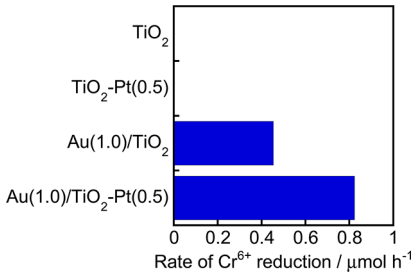

Figure 8. Rates of Cr^{6+} reduction in aqueous suspensions of various photocatalysts under irradiation of visible light from a green LED.

consumed in the case of either TiO_2 or TiO_2−Pt(0.5). These results indicate that visible light coming from the green LED did not cause band gap excitation of TiO_2 and that photocatalysis and/or thermocatalysis of TiO_2−Pt(0.5) were negligible under the present conditions. On the other hand, the Au(1.0)/TiO_2 and Au(1.0)/TiO_2−Pt(0.5) samples were active in Cr^{6+} reduction and showed Cr^{6+} reduction rates of 0.45 and 0.82 μmol h^{-1}, respectively. Loading of Au and Pt particles on the TiO_2 surface without alloying or nanoparticle coagulation was successfully achieved, and a large reaction rate was obtained, as predicted, by the Au(1.0)/TiO_2−Pt(0.5) sample prepared by the combination of the traditional PH method for small Pt cocatalyst particles and the CPH method for large Au particles. Cr^{6+} reduction along with H_2O oxidation under various conditions was examined. Dark reaction in the presence of Au/TiO_2−Pt samples and photochemical reaction gave no or only trace amounts of Cr^{3+} and O_2, although results are not shown. From these results, it can be concluded that Au, TiO_2, and visible light are indispensable for the reduction of Cr^{6+} to Cr^{3+} and the oxidation of H_2O to O_2. Rapid electron transfer from Au to the TiO_2 film under irradiation of visible light was observed using femtosecond transient absorption spectroscopy.[5b]

An expected working mechanism for reduction of Cr^{6+} to Cr^{3+} along with oxidation of H_2O to O_2 over Au/TiO_2−Pt under irradiation of visible light is shown in Scheme 1. Four

Scheme 1. Expected Reaction Mechanism for Reduction of Cr^{6+} and Oxidation of H_2O in Aqueous Suspensions of Au/TiO_2−Pt

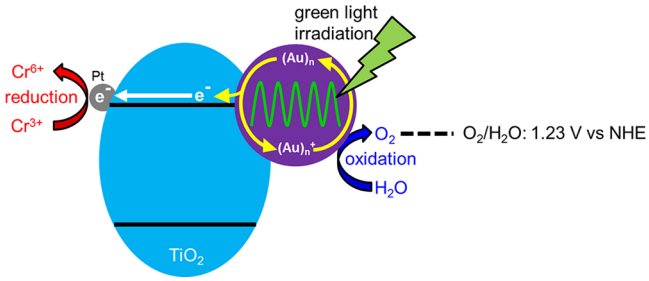

processes would occur: (1) the incident photons are absorbed by Au particles through their SPR excitation,[5,6] (2) electrons are injected from the Au particles into the conduction band of TiO_2, (3) the resultant electron-deficient Au particles oxidize H_2O to O_2 and return to their original metallic state, and (4) electrons in the conduction band of TiO_2 transfer to the Pt nanoparticles as cocatalyst at which reduction of Cr^{6+} to Cr^{3+} occurs. Since the work function of Pt metal (5.40 eV from vacuum[12]) is larger than that of Au metal (4.78 eV from vacuum[12]), that is, the Fermi level of Pt is lower than that of Au, electron transfer from Au to Pt through TiO_2 in processes (2) and (4) is reasonable. Increase in the reaction rate in the presence of Pt nanoparticles is explained by the increased efficiency of charge separation and electron-storage effect for multielectron reduction of Cr^{6+}.

4. CONCLUSIONS

By using traditional photodeposition of Pt cocatalysts on nanocrystalline TiO_2 followed by colloid photodeposition of Au particles onto TiO_2−Pt, Au/TiO_2−Pt samples without alloying Au and Pt and nanoparticle coagulation were successfully prepared. The Au/TiO_2 and Au/TiO_2−Pt samples exhibited strong photoabsorption at around 550 nm due to SPR of Au particles. These photocatalysts reduced Cr^{6+} and oxidized H_2O under irradiation of visible light of a green LED (λ = 540 nm), and the overall reaction was described as $2Cr_2O_7^{2-} + 16H^+ \rightarrow 4Cr^{3+} + 3O_2 + 8H_2O$. Since bare TiO_2 and TiO_2−Pt showed no activity under the same conditions and the apparent quantum yield was in agreement with the subtraction spectrum obtained from the spectra of Au/TiO_2−Pt and TiO_2−Pt, we concluded that SPR photoabsorption of supported Au particles contributed to the simultaneous Cr^{6+} reduction and H_2O oxidation under irradiation of visible light. The Au/TiO_2−Pt sample

dx.doi.org/10.1021/cs400433r | ACS Catal. 2013, 3, 1886−1891

exhibited a rate of O_2 formation about twice larger than that of the Pt-free Au/TiO_2 sample, indicating that Pt nanoparticles loaded on TiO_2 acted effectively as a cocatalyst. The apparent quantum yield reached 1.0% at 550 nm and 0.47% even at 700 nm in the case of Au/TiO_2−Pt. The present Au/TiO_2−Pt sample was easily recovered from the reaction mixture after photoirradiation by simple filtration and was found to be reusable without loss of its activity; the amounts of O_2 formation after irradiation for 24 h were the same in both the second and the third uses of the Au/TiO_2−Pt sample. In addition, photoabsorption of the Au/TiO_2−Pt sample scarcely changed even after this reaction. These results are in contrast to those obtained for the Ag^+ reduction-H_2O oxidation (Ag deposition-O_2 evolution) system using $AgNO_3$ solution in which O_2 formation activity decreased with increase in the number of cycles and photoabsorption of Au/TiO_2−Pt after the reaction was much different from that of the original Au/TiO_2−Pt. The results of two O_2 evolution systems indicate that the present reaction system can be used for evaluation of photocatalytic activity in H_2O oxidation without changes in the photoabsorption property and the activity of the photocatalyst.

AUTHOR INFORMATION

Corresponding Author

*E-mail: hiro@apch.kindai.ac.jp.

Notes

The authors declare no competing financial interest.

ACKNOWLEDGMENTS

This work was partly supported by a Grant-in-Aid for Scientific Research (No. 23560935) from the Ministry of Education, Culture, Sports, Science, and Technology (MEXT) of Japan. One of the authors (A. T.) appreciates the Japan Society for the Promotion of Science (JSPS) for a Research Fellowship for young scientists.

REFERENCES

(1) Bard, A. J.; Fox, M. A. *Acc. Chem. Res.* **1995**, *28*, 141−145.

(2) (a) Kudo, A.; Miseki, Y. *Chem. Soc. Rev.* **2009**, *38*, 253−278. (b) Abe, R. *J. Photochem. Photobiol. C* **2010**, *11*, 179−209. (c) Maeda, K.; Lu, D.; Domen, K. *Chem.—Eur. J.* **2013**, *19*, 4986−4991.

(3) (a) Nakamura, R.; Okamura, T.; Ohashi, N.; Imanishi, A.; Nakato, Y. *J. Am. Chem. Soc.* **2005**, *127*, 12975−12983. (b) Silva, C. G.; Bouizi, Y.; Fornes, V.; Garcia, H. *J. Am. Chem. Soc.* **2009**, *131*, 13833−13839.

(4) Kominami, H.; Yabutani, K.; Yamamoto, T.; Kera, Y.; Ohtani, B. *J. Mater. Chem.* **2001**, *11*, 3222−3227.

(5) (a) Tian, Y.; Tatsuma, T. *J. Am. Chem. Soc.* **2005**, *127*, 7632−7637. (b) Furube, A.; Du, L.; Hara, K.; Katoh, R.; Tachiya, M. *J. Am. Chem. Soc.* **2007**, *129*, 14852−14853. (c) Naya, S.; Teranishi, M.; Isobe, T.; Tada, H. *Chem. Commun.* **2010**, *46*, 815−817. (d) Kowalska, E.; Abe, R.; Ohtani, B. *Chem. Commun.* **2009**, 241−243. (e) Kowalska, E.; Mahaney, O. O. P.; Abe, R.; Ohtani, B. *Phys. Chem. Chem. Phys.* **2010**, *12*, 2344−2355. (f) Yuzawa, H.; Yoshida, T.; Yoshida, H. *Appl. Catal., B* **2012**, *115*, 294−302. (g) Ke, X.; Sarina, S.; Zhao, J.; Zhang, X.; Chang, J.; Zhu, H. *Chem. Commun.* **2012**, *48*, 3509−3511. (h) Wang, G.; Wang, X.; Liu, J.; Sun, X. *Chem.—Eur. J.* **2012**, *18*, 5361−5366.

(6) (a) Kominami, H.; Tanaka, A.; Hashimoto, K. *Chem. Commun.* **2010**, *46*, 1287−1289. (b) Kominami, H.; Tanaka, A.; Hashimoto, K. *Appl. Catal., A* **2011**, *397*, 121−126. (c) Tanaka, A.; Hashimoto, K.; Kominami, H. *ChemCatChem* **2011**, *3*, 1619−1623. (d) Tanaka, A.; Hashimoto, K.; Kominami, H. *Chem. Commun.* **2011**, *47*, 10446−10448. (e) Tanaka, A.; Sakaguchi, S.; Hashimoto, K.; Kominami, H. *Catal. Sci. Technol.* **2012**, *2*, 907−909. (f) Tanaka, A.; Hashimoto, K.; Kominami, H. *J. Am. Chem. Soc.* **2012**, *134*, 14526−14533. (g) Tanaka, A.; Ogino, A.; Iwaki, M.; Hashimoto, K.; Ohnuma, A.; Amano, F.; Ohtani, B.; Kominami, H. *Langmuir* **2012**, *28*, 13105−13111. (h) Tanaka, A.; Sakaguchi, S.; Hashimoto, K.; Kominami, H. *ACS Catal.* **2013**, *3*, 79−85. (i) Tanaka, A.; Nishino, Y.; Sakaguchi, S.; Yoshikawa, T.; Imamura, K.; Hashimoto, K.; Kominami, H. *Chem. Commun.* **2013**, *49*, 2551−2553. (j) Tanaka, A.; Hashimoto, K.; Ohtani, B.; Kominami, H. *Chem. Commun.* **2013**, *49*, 3419−3421.

(7) Yoneyama, H.; Yamashita, Y.; Tamura, H. *Nature* **1979**, *282*, 817−818.

(8) Barrera-Diaza, C. E.; Lugo-Lugo, V.; Bilyeu, B. *J. Hazard. Mater.* **2012**, *223−224*, 1−12.

(9) Frens, G. *Nat. Phys. Sci.* **1973**, *241*, 20−22.

(10) Clesceri, L. S., Greenberg, A. E., Eaton, A. D., Eds.; *Standard Methods for the Examination of Water and Wastewater*, 20th ed.; American Public Health Association: Washington, DC, 1998.

(11) Maeda, K.; Domen, K. *Angew. Chem., Int. Ed.* **2012**, *51*, 9865−9869.

(12) Trasatti, S. *J. Electroanal. Chem.* **1971**, *33*, 351−378.